Combined automatic segmentation of fat and muscle compartments with T1 and T2* measurements using a triple-angle multiple gradient-echo acquisition technique

Benjamin Leporq[1], Yann Le Fur[2], Patrick Cozzone[2], Olivier Beuf[1], and David Bendahan[2]

[1]CREATIS; CNRS UMR 5220; INSERM U1044; INSA-Lyon; UCBL Lyon 1, Villeurbanne, Rhône-Alpes, France, [2]CRMBM; CNRS UMR 6612; Université Aix-Marseille, Marseille, PACA, France

INTRODUCTION

Due to its sensitivity to key processes occurring in diseased muscle such as oedema/inflammation and fat infiltration, MRI is emerging as a suitable quantitative method which could provide reliable surrogate markers of disease severity and progression (1,2). In contrast to muscle biopsy, which provides anatomo-pathological information from a limited amount of superficial tissue, MRI offers a repeatable, non-invasive, whole-organ approach which should provide useful indices of muscle disease processes. Regarding the fatty infiltration commonly reported in diseased muscle, several approaches have been developed in order to quantify the water/fat ratio. Automatic processes of conventional MR images using contrast thresholds have been reported but they did not provide an accurate information related to the microscopic fat infiltration (3,4). Dixon techniques providing information about the individual contribution of fat and water in each voxel have also been used but T_1 and T_{2*} relaxation processes may introduce quantitative biases. Quantitative methods based on relaxation times measurements such as single T_2*-IDEAL or low flip angle multiple gradient echoes (5-7) have been reported for proton density fat fraction (PDFF) quantification, especially in the liver. The aim of the present study was to evaluate the feasibility of 3D segmentation of fat and muscular tissue using a triple-angles multiple gradient-echo acquisition. Our approach included a complex-based technique for fat volume fraction (FVF) quantification with independent measurements of fat and water T_1 and T_2*, and corrections related to T_1 bias and spectral complexity of fat. The measurements were performed in healthy subjects at 1.5T.

MATERIAL and METHOD

Subjects: Five healthy subjects (mean age: 35.8 ± 9.2 years; mean weight: 73.0 ± 9.1 Kg) were enrolled after informed consent was obtained.

MR acquisition: Acquisitions were performed at 1.5T (*Magnetom Avanto, Siemens Medical Solutions, Erlangen, Germany)*. A FLASH 3D sequence was repeated three times with 5, 10 and 15° flip angles. The choice of the flip angles values was done according to T_1-values and TR values. Acquisition parameters were : 4 first Out-of-Phase (OP) echoes and 4 first In-Phase (IP) echoes; TR/TE = 22/n × 2.38 ms with n ranging from 1 to 8, 128 × 256 matrix; 180 × 360 mm^2 FOV; 454 Hz.pixel^{-1} bandwidth, 2 averages and 32 slices of 4 mm thickness in the axial plane.

Post-processing: All post-processing steps were performed using an in-house developed application on Matlab r2010a (*The MathWorks, Natick, MA, USA*).

First step - 2D FVF mapping: For each echo, magnitude and phase images were used to calculate real signal images after phase unwrapping. Initially, separation of fat and water signal magnetizations at t=0 (M_{0fat} and M_{0water}) was done from the T_1-weighted images using a 2-parameters interference bi-exponential model. Then, apparent T_1 (T_{1app}) assuming a mono exponential signal (single component) was estimated from the first IP images acquired with the two angles. Because T_1 of fat (T_{1fat}) is almost invariant, it was fixed at 250 ms and then T_1 of water (T_{1water}) was calculated as: $T_{1water} = (T_{1app} - (M_{0fat}/(M_{0water} + M_{0fat})) \times T_{1fat}) / (1-(M_{0fat}/(M_{0water} + M_{0fat})))$. This relation was experimentally verified from fat and doped water mixture phantoms with measurement of pure water T_1-values, pure fat T_1-values and equally-mixed fat-water T_1-values. Finally, quantification of proton density fat fraction (PDFF) was performed using a 4-parameter dual-T_2* bi-exponential model including a T_1 correction from previous estimated T_1-values and fat spectral modeling with the five main fat peaks (0.9-1.3-2.1-4.2 and 5.3 ppm) as described by Hamilton *et al* (8). Fat volume fraction (FVF) was then computed from the following formulae: $FVF = PD_f / (k \times PD_w + PD_f)$ were k is a scaling coefficient (k = 0.95) illustrating the relative difference between proton density of fat and water as described by Reeder *et al*. (9). The fitting processes were performed pixel-by-pixel using the Levenberg-Marquardt algorithm and multi-start technique to improve fit robustness. Five parametric maps (T_1 recombined, T_2* recombined, fat PD, water PD and fat volume fraction) were generated for each slice.

Second step – 3D Segmentation of fat and muscular tissue: Segmentation was performed on 15° flip angle first IP images using a segmentation mask built from the FVF map and a threshold value fixed. A semi-automatic method was used to erase the bone marrow from each image. Then, 3D volume of subcutaneous fat and 3D volume of muscular tissue were built from 2D segmented images. Mean T2* and T1-values for fat and muscle were calculated based on segmented volumes with FVF.

RESULTS

Mean muscle tissue and fat volumes calculated (with FVF threshold values set to 50%) on all subjects were 6828 ± 265 cm^3 and 1077 ± 223 cm^3 respectively with 13.6 ± 8.7% mean fat fraction. Mean T_2* and T_1-values were 26.8 ± 1.4 ms and 1059 ± 30.1 ms respectively for the muscle compartment whereas they were much shorter for the fat compartment i.e. T_2* = 13.4 ± 0.7 ms and T_1 = 278 ± 13.9 ms. Inter-subject relative standard variation was 2.9%, 5.2%, 5.0% and 5.2% for T_1-value of muscular tissue, T_2*-value of muscular tissue, T_1-value of fatty tissue and T_2*-value of fatty tissue respectively. Based on 40 measurements from 2D FVF map, FVF were 93.4 ± 4.3%: 97.0 ± 4.5% and 2.1 ± 2.1% on subcutaneous region, bone marrow and muscular tissue respectively.

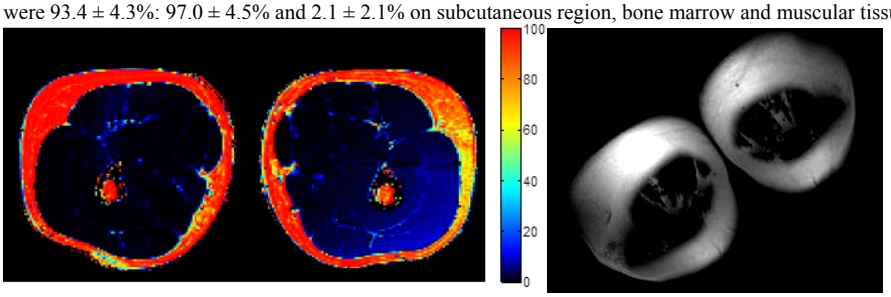

Fig.1 : Exemple of 2D FVF map used to define segmentation mask based on a threshold value (left) and 3D rendering of the segmented fat tissue volume (right).

DISCUSSION

FVF measured on subcutaneous fat region as well as estimated muscular T_1-values were similar to that encountered in the literature (10,11). Among this healthy subject group, relative standard variation for each quantified parameters was reasonable (between 2.9 and 4.8%). All these features demonstrate the accuracy of FVF quantification algorithm and the reproducibility of this method. As values of quantifiable FVF can scale between 0 and 100% (>50%), the use of complex-based approach was required. A slight overestimation of muscle FVF (2% instead of 0%) was found probably due to the absence of noise bias and eddy-current correction. As described by Reeder et al (11), these effects encountered with complex-approach only, could provide overestimated FVF, especially for the small values. In this context, this is a minor limitation because FVF of fat infiltration or subcutaneous tissues are expected to be higher than a few percent. In conclusion, we reported a robust method allowing to quantify the FVF in the thigh muscles taking into account different confounding factors related to fat and water respectively. The corresponding FVF-maps provide an accurate 3D segmentation of subcutaneous tissue in healthy subjects and could be used in order to quantify macroscopic or microscopic fatty infiltration in patients with muscle disorders. In addition, we obtained relevant measurements of muscular tissue relaxation times (T_1 and T_2*). We investigated FVF and T_1 and T_2* in healthy subjects and similar measurements performed in diseased muscle should provide reliable indices of disease severity and progression.

REFERENCES

[1] Mercuri *et al*. JMRI 2007;25:433-40.
[2] Wren TAL *et al*. AJR 2008;190:W8-W12.
[3] Mattei *et al*. Magma 2006;19:275-79.
[4] Positano *et al*. JMRI 2009;29:677-84.
[5] Hussain HK *et al*. Radiology 2005;237:1048-105.
[6] O'Regan DP *et al*. Radiology 2008;247
[7] Yokoo *et al*. Radiology 2009;251:67-76
[8] Hamilton G *et al*. NMR Biomed 2010.
[9] Reeder SB *et al*. ISMRM 2009 proceedings
[10] De Bazelaire CMJ *et al*. Radiology 2004;230:652-59
[11] Reeder SB *et al*. JMRI 2011;34:729-49.